Chapter 3
Mechanism of Gas Transport through a Supported Silica Membrane

3.1. Introduction

In this chapter, the permeation characteristics of the gas molecules, He, Ne, H_2, CO_2, CO, and CH_4, on Vycor glass and the Nanosil membrane are presented in more detail. The results are discussed applying existing gas transport theories and a new treatment developed in this work. It was found that the gas permeation mechanism on the Vycor glass follows a surface-diffusion-enhanced Knudsen permeation model, whereas the mechanism on the Nanosil membrane obeys a statistical solid-state diffusion model. The model is able to rationalize the unusual order of permeability, He > H_2 > Ne, which does not follow either molecular weight or size.

3.2. Experimental

The Nanosil membrane was prepared by depositing a thin silica layer on a porous Vycor support by the chemical vapor deposition (CVD) of tetraethylorthosilicate (TEOS) at 873 K in an argon stream. Vycor glass (7930 glass, Corning, Inc.) with a nominal average pore size of 4 nm was used as a substrate for the silica deposition. It had a tubular geometry with an outside diameter of 10 mm and a thickness of 1 mm. A 4 cm section of the Vycor glass was connected to two pieces of quartz tubing by glassblowing joints. This tubular ensemble was placed concentrically inside another piece of tubing of 14 mm inside diameter using machined Swagelok fittings with Teflon ferrules. After placing the assembly in an electric furnace, argon gas flows were introduced on the outer shell side (20 μmol s^{-1}) and inner tube side (8 μmol s^{-1}) of the reactor (flow rates in μmol s^{-1} may be converted to cm^3 min^{-1} (NTP) by multiplying by 1.5), and the temperature was raised to 873 K. A flow of tetraethylorthosilicate (TEOS, Aldrich, 98%) was introduced on the inside of the Vycor substrate through a bubbler (at 298 K) using argon (3 μmol s^{-1}) as a carrier gas. This stream was premixed with the tube stream of argon

before introducing it to the tube side to produce a stream with a TEOS concentration of 0.03 mol m^{-3} (0.07 mol %).

The synthesis of the Nanosil membrane was studied by varying the silica deposition time. The CVD process was interrupted at various times (3, 6, 9, 12 h) and the permeation rates of gases were measured at each deposition time at 873 K.

General gas permeation measurements were conducted in the temperature range of 300 – 873 K by flowing 20 μmol s^{-1} of a pure gas at 123 kPa in the outer shell side. The permeation rate of each gas exiting from the inside of the membrane tube was measured with a sensitive bubble flow meter at atmospheric pressure. The permeance of gas was obtained from $Q_i = F_i / A \Delta P$, where Q_i is the permeance (mol m^{-2} s^{-1} Pa^{-1}), F_i is the gas flow rate on the tube side (mol s^{-1}), A is the surface area (m^2) of the membrane section, and ΔP is the pressure difference (Pa) between the shell and tube side.

For higher sensitivity the permeance of the gases was also measured with a gas chromatograph (GC) equipped with a thermal conductivity detector (SRI, Model 8610B). The shell side gas flow rates and pressure conditions were the same as above, however, on the tube side an argon flow was introduced as a sweep gas for the permeated gas. The tube side outlet gas flow rate was measured using a bubble flow meter, and the flow was injected into the GC to obtain the concentration of the permeated gas. The permeance was then calculated using the outlet gas flow rate and the concentration of the permeated gas on the tube side.

3.3. Gas Transport through the Membranes

There have been many studies associated with gas transport through membranes, and extensive discussions can be found in the literature [1-6]. A variety of models have been used to describe the transport through membranes such as porous glass [1,2], zeolites [3,5], alumina and silica [6]. These models have different theoretical bases associated with the details of the gas diffusion mechanism. Sorption and diffusion are two major process that play important roles in the overall gas transport, where sorption describes the interactions between gas molecules and

the membrane surface, and diffusion describes the rate of gas passage through the membrane. Qualitative and quantitative analysis of the involvement of these steps is required to understand the overall gas transport mechanism since each process can contribute to the total permeation rate, and its importance will differ according to such variables as temperature, pressure, and composition.

Sorption of gas molecules from the bulk gaseous state to the surface of the membranes can occur physically or chemically depending on the nature of the force between the gas molecules and the surface. Chemisorption occurs when the interactions are strong, for example, in the dissociative adsorption of hydrogen molecules on palladium membranes [7]. Physisorption occurs when the interactions with the surface are weak, for example, in the adsorption of CO_2 on microporous glass membranes [8]. In the subsequent transport process the adsorbed molecules diffuse through the membrane in various way under the driving force of a concentration gradient. Detailed discussion of these sorption and diffusion steps follows in the next sections

3.3.1. Theoretical Background

Fick's first law applies for the macroscopic description of transport process,

$$J = -D(c)\nabla c \tag{3.1}$$

where J is the flux (mol m^{-2} s^{-1}), D(c) is the concentration dependent diffusivity (m^2 s^{-1}), and c is the concentration (mol m^{-3}).

3.3.1.1. Sorption

Gas transport through microporous or dense materials such as zeolites or bulk solid oxides requires adsorption of molecules before the subsequent diffusion process. Numerous sorption models have been reported in the literature based on different assumptions about the state of the adsorbed gas [9]. In membrane applications for gas separation, adsorption is usually not multilayer, and often well below a monolayer, so is well described by the Langmuir adsorption model [10].

$$\theta = \frac{q}{q_S} = \frac{b\,P}{1 + b\,P} \tag{3.2}$$

where θ is the fractional occupancy of adsorption sites, q is the amount of adsorbed gas molecules per unit mass of adsorbent (mol g^{-1}), q_s is the saturation amount of adsorbed molecules, P is the pressure (Pa) and b is an equilibrium adsorption constant (Pa^{-1}). The dependency of the equilibrium adsorption constant on temperature is given by,

$$b = b_0 \exp\left(\frac{\Delta H_a}{RT}\right) \tag{3.3}$$

where ΔH_a is the heat of adsorption. At low pressure and high temperature (small values of b), the Langmuir equation may be simplified to,

$$q = q_s\, b\, P = K\ P = K_0 \exp\left(\frac{\Delta H_a}{RT}\right) P \tag{3.4}$$

where K is a Henry's constant (mol g^{-1} Pa^{-1}). In the Henry's law regime the amount of adsorbed molecules increases linearly with applied pressure.

3.3.1.2. Diffusion

Diffusion of molecules through a membrane can proceed in various ways depending on the nature of the interaction between the diffusing gas molecules and the membrane. Various gas diffusion processes were discussed by Burggraaf [3] in terms of the associated energy potential wells developed inside the pores of membrane. The shapes of these energy potential wells depend mainly on the distance between the pore walls and the diffusing gas molecules. Therefore, the ratio of the molecular size of the diffusing gas and the pore diameter plays a major role in determining which diffusion mechanism may apply. We will discuss four different gas diffusion mechanisms (Knudsen, gas translational (GT), solid state, and surface diffusion) that are often involved in gas transport through membranes.

Knudsen diffusion occurs when the mean free path of the diffusing gas molecules is much larger than the pore size [11]. In this regime the gas molecules pass through the pores

undergoing random collisions with the pore walls, and the Knudsen diffusivity is obtained from the gas kinetic velocity and the geometric parameters associated with the membrane.

$$D = \frac{\varepsilon d_p}{3\tau}\left(\frac{8RT}{\pi M}\right)^{\frac{1}{2}} \tag{3.5}$$

where ε is the porosity of the membrane, d_p is the pore diameter, τ is the tortuosity, R is the gas constant and M is molecular weight of the diffusing gas.

The gas translational (GT) diffusion mechanism has been applied to microporous materials such as zeolites [3,5]. The expression obtained is similar to the Knudsen equation, but in this model the gas molecules are considered to move between sorption sites (cages) in a translational mode by overcoming the obstructions formed by the small channels that connect adjacent sorption sites. The GT diffusivity is given by,

$$D = g_d\, d_p \left(\frac{8RT}{\pi M}\right)^{\frac{1}{2}} \exp\left(-\frac{\Delta E}{RT}\right) \tag{3.6}$$

where g_d is a geometric factor, d_p is the pore size of the material and ΔE is the activation energy of diffusion. The activation energy is considered to be the difference between the potential energy in the sorption sites and in the channels of the zeolites.

As the ratio of the pore size of the membrane versus the size of the diffusing gas molecule decreases, the energy potential in the pores will develop into a steep parabolic potential where the movement of gas molecules changes from a translational to a vibrational mode. A bound molecule in one sorption site will jump to other sorption sites with a vibrational frequency, ν_e, and a jump length, λ. In this regime the gas diffusion is similar to solid state diffusion, and the diffusivity is given by [3]:

$$D = g_d\, \lambda^2\, \nu_e\, \exp\left(-\frac{\Delta E}{RT}\right) \tag{3.7}$$

where g_d is a geometric constant and ΔE is the activation energy of diffusion. A model for solid state diffusion also can be obtained by a statistical approach. For gas diffusion in fused silica glass, a statistical model of monatomic gas diffusivity is given by [12]:

$$D = \frac{1}{6}\left(\frac{kT}{h}\right) d^2 \frac{(e^{h\nu/2kT} - e^{-h\nu/2kT})^3}{(e^{h\nu^*/2kT} - e^{-h\nu^*/2kT})^2} e^{-\Delta E/RT} \quad (3.8)$$

where k is Boltzmann's constant, h is Planck's constant, d is the distance between sorption sites in the structure, T is the absolute temperature, n is the vibrational frequency of gas molecules on the sorption sites, n* is the vibrational frequency on the doorway sites, R is the gas constant, and DE is the activation energy of diffusion.

Surface diffusion can be expressed in the same way as solid state diffusion except that the model equation obtained has a 2-dimensional physical meaning. In surface diffusion gas molecules are considered to be adsorbed on the surface and to move on the surface by hopping between the potential minima produced on the pore surface [3]. However, the diffusing gas molecules bound on the surface may escape from their adsorbed state to the gaseous state if their kinetic energy is larger than their sorption energy. Thus, surface diffusion is only applicable in a relatively low temperature range that depends on the sorption energy of the gas molecules. Also, the activation energy for surface diffusion is lower than the sorption energy.

3.3.1.3. Permeation

The flux (mol m^{-2} s^{-1}) of gas transport through the membranes is obtained using Fick's first law. In gas phase membrane applications permeance and permeability are usually used as measures of gas transport rate. The permeance, *Q*, (mol m^{-2} s^{-1} Pa^{-1}) is defined as the flux per unit pressure difference between the two sides of the membrane. If the thickness of the separation layer of the membranes is known, the permeability coefficient, *P*, (mol m^{-1} s^{-1} Pa^{-1}) is obtained by normalizing the permeance by the unit thickness of the separation layer.

Gas transport by Knudsen diffusion occurs in the gaseous state without involvement of adsorption. Therefore, the molar flux (mol m^{-2} s^{-1}) can be obtained using the Knudsen diffusivity and Fick's first law, where the concentration is obtained using the ideal gas law. The Knudsen permeance is then given by,

$$Q = \frac{\varepsilon\, d_p}{\tau L}\left(\frac{8}{9\pi M R T}\right)^{\frac{1}{2}} \tag{3.9}$$

where L is the thickness of the membrane.

In many cases of gas permeation through microporous membranes, gas molecules adsorb on the membranes. This adsorption is followed by diffusion to the opposite side of the membranes where the molecules desorb to the gaseous state. In Henry's law regime the amount of adsorption on the membrane is linearly proportional to the partial pressure (Eq. 3.4). Therefore, the permeance is obtained using the diffusivity and Henry's constant (K).

$$Q = \frac{\rho\, \varepsilon}{L} D_0(q)\, K_0 \exp\left(\frac{\Delta H_a}{RT}\right)\exp\left(\frac{-\Delta E}{RT}\right) = Q_0 \exp\left(\frac{\Delta H_a - \Delta E}{RT}\right) \tag{3.10}$$

where ρ is the density of the membrane (g m^{-3}).

There also have been a few statistical studies describing adsorption and diffusion of gas molecules through vitreous silica glass [12-14]. The solubility (mol m^{-3} Pa^{-1}), *S*, of small gases in the silica glass is given by [14]:

$$S = \frac{n_s}{N_A P} = \left(\frac{h^2}{2\pi m k T}\right)^{\frac{3}{2}} (kT)^{-1} \frac{N_S}{N_A}\left(\frac{e^{-h\nu/2kT}}{1 - e^{-h\nu/kT}}\right)^3 e^{E(0)/RT} \tag{3.11}$$

where n_s is the number of gas molecules dissolved per m^3 of glass volume, P is the applied gas pressure, m is the mass of the molecule, h is Planck's constant, k is Boltzmann's constant, ν is the vibrational frequency of gas molecules on the sorption sites, T is temperature, N_s is the number of solubility sites available per m^3 of glass volume, N_A is Avogadro's number, R is the gas constant, and E(0) is the binding energy of the physically dissolved gas molecule in an interstitial sorption site. The permeability, *P*, of a monatomic gas through silica glass is obtained by using the solubility equation (Eq. 3.11) and the diffusivity equation (Eq. 3.8), and the permeance is obtained by including the thickness of the separation layer, L, in the permeability equation [12].

$$Q = \frac{1}{6L}\left(\frac{d^2}{h}\right)\left(\frac{h^2}{2\pi m k T}\right)^{\frac{3}{2}} \frac{(N_S/N_A)}{(e^{h\nu^*/2kT} - e^{-h\nu^*/2kT})^2}\, e^{-\Delta E_K/RT} \tag{3.12}$$

where the ΔE_K is the activation energy for the permeation. In the case of polyatomic molecules rotational partition functions on the solubility site and sorption site are also considered in the model equation.

3.4. Results and Discussion

Two types of membrane were studied in this work. One was a commercial Vycor glass, and the other was a supported type membrane consisting of a thin layer of silica deposited on Vycor. The N_2 adsorption/desorption isotherms for the two membranes are shown in Figure 3.1. The shape of the isotherms (type IV) and desorption curves indicate that the materials are microporous with pore shapes that are slit like. The total pore volume was 0.18 $cm^3\ g^{-1}$, and the average pore size was 3.6 nm. The latter value agreed well with the manufacturer's nominal pore size of 4.0 nm. The pore size distribution curves obtained from the nitrogen desorption isotherm using the Barrett, Joyner and Halenda (BJH) method of the fresh Vycor and Nanosil membrane are presented in Figure 3.2. There was little change in the pore size distribution by the deposition of the silica layer indicating that it was deposited on the outer surface of the Vycor glass without significant penetration into the pore structure.

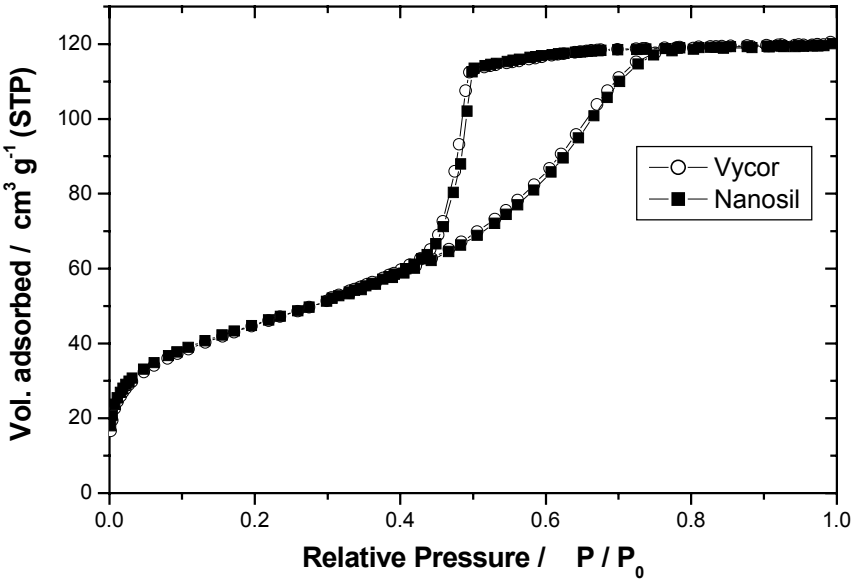

Figure 3.1. Nitrogen adsorption/desorption isotherms for the Vycor and Nanosil membrane

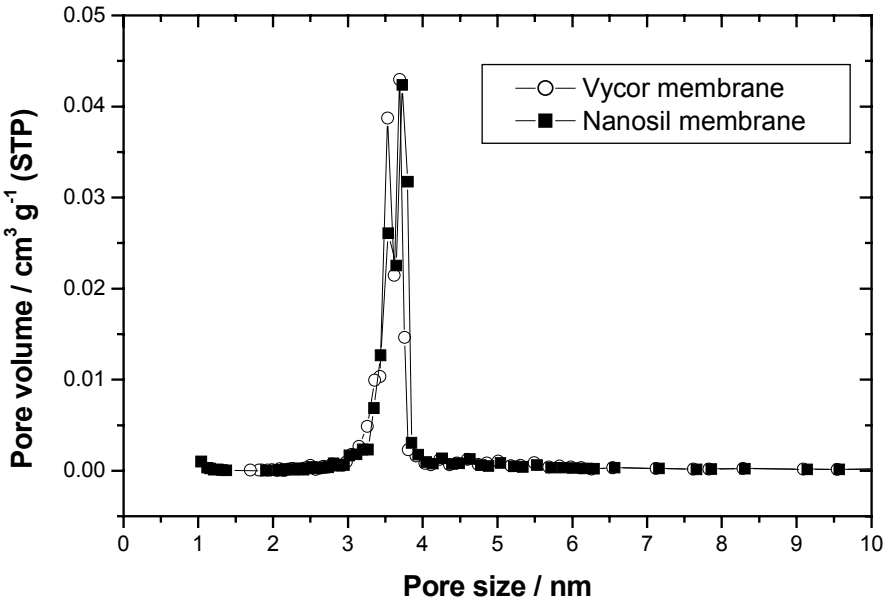

Figure 3.2. Pore size distributions of the Vycor and Nanosil membrane

3.4.1. Permeance of the Vycor Glass Membrane

The ratio of the mean free path of the diffusing gases (He, Ne, H_2, CH_4, CO and CO_2) and the pore size of the Vycor glass (3.6 nm) falls between 50 and 110 (at 873 K and 1 bar) [15]. Since the mean free paths of the gases are much larger than the pore size of Vycor glass, transport through the membrane has generally been described by the Knudsen diffusion mechanism [16,17].

A characteristic feature of gas transport by the Knudsen mechanism is that permeance shows an inverse square root dependence on temperature and molecular weight of the diffusing gas molecule (Eq. 3.9). Therefore, every diffusing gas should have the same value of $Q \times (MT)^{1/2} = \frac{\varepsilon d_p}{\tau L}\left(\frac{8}{9\pi R}\right)^{\frac{1}{2}}$ independent of temperature if gas transport through the membrane involved only Knudsen diffusion. Gas permeance data on Vycor glass analyzed in this manner are shown in Figure 3.3. Relatively constant values of $Q \propto (MT)^{1/2}$ for Ne, He and H_2 over the

applied temperature range in this study indicate that the transport of these gases through the Vycor membrane takes place mainly by the Knudsen diffusion mechanism.

The permeance data for Ne, He, and H_2 was fitted to the Knudsen permeance model (Eq. 3.9) by the least squares method. Values of the group, $C=\frac{\varepsilon d_p}{\tau L}\left(\frac{8}{9\pi MR}\right)^{\frac{1}{2}}$, of the Knudsen model were calculated using the geometric parameters of Vycor glass, $\varepsilon = 0.28$ [17,18], $\tau = 5.9$ [19], $d_p = 3.6\times10^{-9}$ m, and $L = 1.0\times10^{-3}$ m, and a comparison with the experimentally determined values is shown in Table 3.1. The results show good agreement between the experimental and model calculation for the groups indicating the applicability of the Knudsen mechanism for these gases.

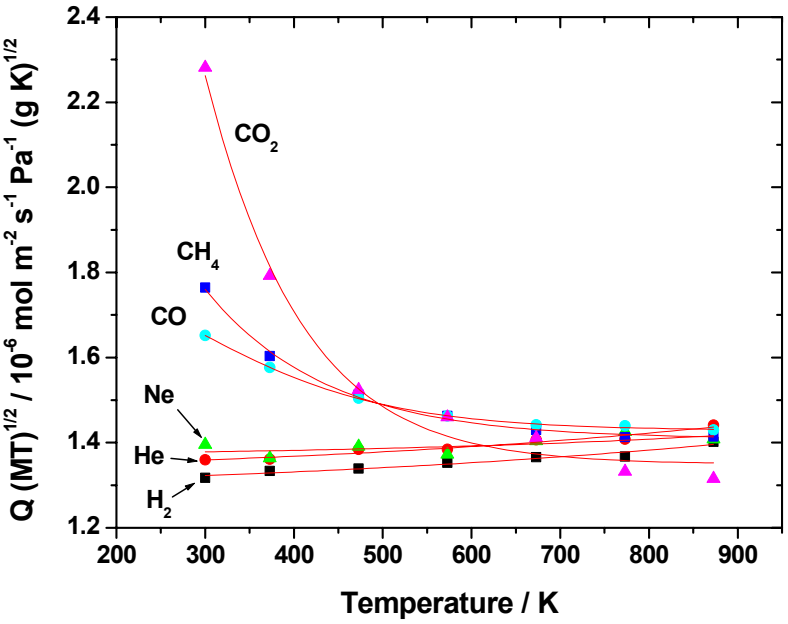

Figure 3.3. $Q \times (MT)^{1/2}$ vs. temperature for the Vycor membrane

The results for CH_4, CO and CO_2 differ from those for He, Ne and H_2. For the heavier gases the values of $Q \times (MT)^{1/2}$ for CH_4, CO and CO_2 increase as temperature decreases indicating that the transport is not entirely by the Knudsen mechanism at lower temperatures. The results for these

heavier gases can be explained by the occurrence of surface diffusion at low temperatures. As temperature decreases the contribution of

Table 3.1. Values of the parameters for the Knudsen model

Gas	n	C (exptl.) mol $K^{½}/m^2sPa$	C (calc.) mol $K^{½}/m^2sPa$	Sum of least squares $\Sigma (Q_{cal.} - Q_{expl.})^2$
He	-0.449	5.04×10^{-7}	4.98×10^{-7}	1.3×10^{-18}
Ne	-0.476	2.67×10^{-7}	2.22×10^{-7}	3.8×10^{-17}
H_2	-0.451	7.01×10^{-7}	7.02×10^{-7}	3.6×10^{-19}

surface diffusion increases due to an increase in adsorption [1]. The Knudsen diffusion and surface diffusion processes occur in parallel, and the permeance for the adsorbable gases is given by,

$$Q\,(\text{Vycor}) = Q\,(\text{Knudsen}) + Q\,(\text{Surface}) \qquad (3.13)$$

The Knudsen permeance of CH_4, CO and CO_2 were calculated using the model equation (Eq. 3.9), and are compared with the experimental permeance data in Figure 3.4. The results show that the permeance of the adsorbable gases through the Vycor is higher than the expected Knudsen permeance over the entire temperature range studied. The contribution of surface diffusion to the overall gas permeance through the Vycor is significant for the adsorbable gases even at high temperatures. At 300 K the experimental gas permeance is between 1.7 and 2.4 times higher than the expected Knudsen permeance, while at 873 K it is about 1.4 times higher.

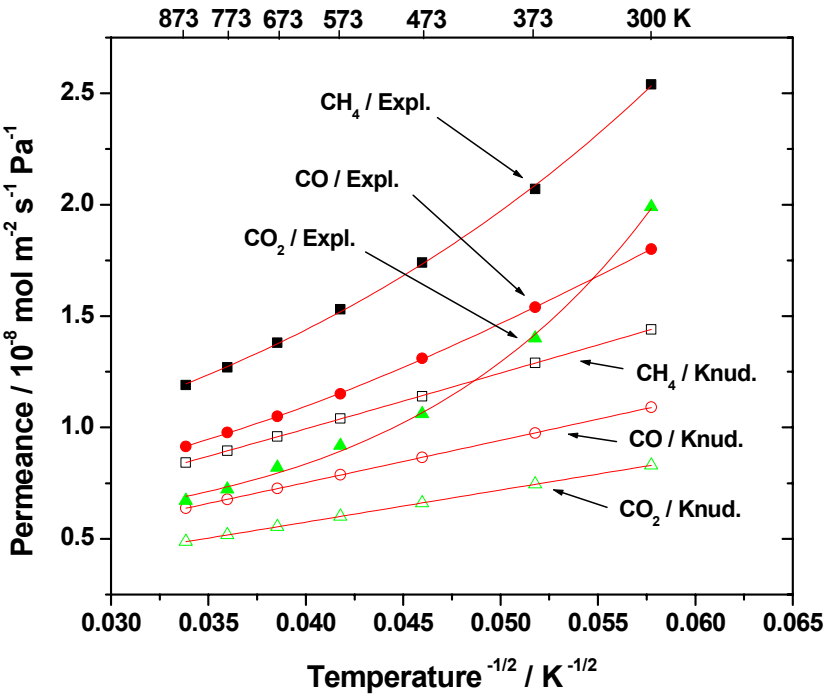

Figure 3.4. Model-calculated and experimental gas permeance on the Vycor membrane

The gas permeance by surface transport on the Vycor was obtained by subtracting the calculated Knudsen permeance from the experimental permeance data using Eq. 3.13. The obtained permeance was then analyzed using the sorption-diffusion gas transport model equation (Eq. 3.10). The results plotted in Arrhenius form (Eq. 3.10) are shown in Figure 3.5. The best-fit parameters are shown in Table 2. The results clearly show good agreement between the predicted equation for activated diffusion and the experimental gas transport on the Vycor membrane.

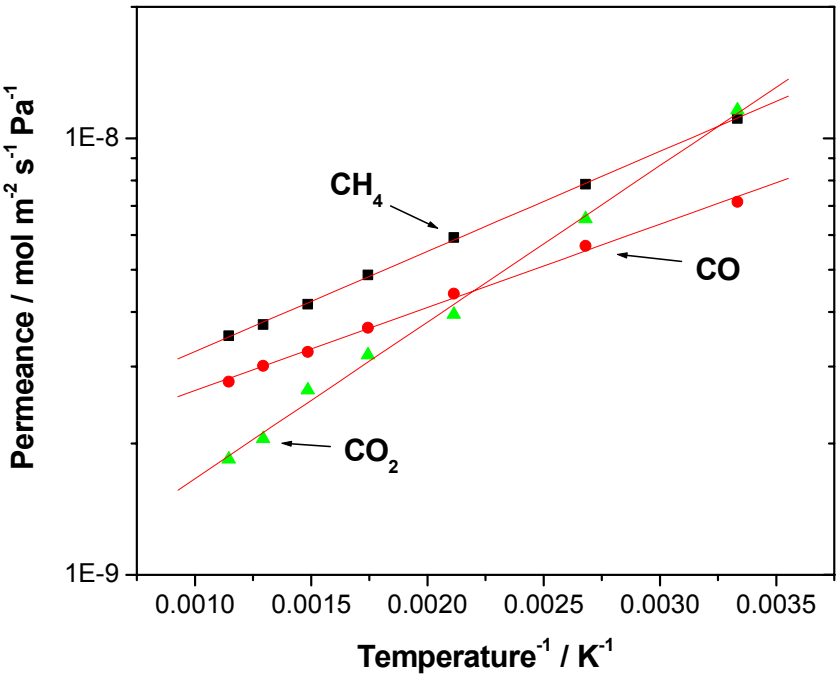

Figure 3.5. Surface transport of CH_4, CO, and CO_2 through the Vycor membrane

Table 3.2. Values of the model parameters for surface diffusion on Vycor

Gas	Q_0 (mol m^{-2} s^{-1} Pa^{-1})	$\Delta H_a - \Delta E$ (kJ mol^{-1})	Regression coefficient
CH_4	1.92×10^{-9}	4.4	0.9997
CO	1.71×10^{-9}	3.7	0.9984
CO_2	7.28×10^{-10}	6.9	0.9980

3.4.2. Permeance of the Nanosil Membrane

To investigate the formation of the Nanosil membrane by the deposition of silica on the Vycor, the evolution of gas permeance was measured as a function of the silica deposition time. The results are shown in Figure 3.6. After 12 h of silica deposition the permeance of the small gas molecules He, Ne and H_2 decreased slightly from the permeance on the fresh Vycor support. However, the permeance of CH_4, CO and CO_2 showed an abrupt drop after 6 hours of silica deposition and significant further reduction after 9 hours. Initially, the permeance order for these gases followed an inverse square root of molecular weight dependency, $CH_4 > CO > CO_2$, in agreement with a Knudsen mechanism. However, after the drop the order changed to $CO_2 > CO > CH_4$ which follows molecular size (CO_2 = 0.33 nm, CO = 0.376 nm, CH_4 = 0.38 nm [20]). This gives evidence that the mechanism of molecular differentiation by the silica layer is through size selectivity. The species He, Ne and H_2 have smaller size (He = 0.26 nm, Ne = 0.275 nm, H_2 = 0.289 nm [20]) and therefore can continue to permeate. The remarkable finding was that after 12 hours of silica deposition, the permeances of CO_2, CO and CH_4 were unmeasurable by thermal conductivity detector (TCD) measurements whereas the experimental H_2, He and Ne permeance were scarcely affected. Taking into account the detection limits of the TCD, it was concluded that the H_2 selectivity over CO_2, CO and CH_4 is over 10,000. The ability of the Nanosil membrane to separate H_2 from other large gas molecules with practically 100 % selectivity and a high permeance comparable to the permeance on the support is unprecedented for silica based membranes.

In the previous chapter, the atomic force microscopy (AFM) images of the Vycor and the Nanosil membrane surface were reported. The thickness of the silica layer deposited on the Vycor was deduced to be approximately 10 nm from the change in surface topology after the silica deposition. Therefore, it appears that the unusually high H_2 selectivity on the Nanosil membrane originates from the thin, defect-free SiO_2 layer, with only the small gas molecules (He, Ne and H_2) being able to pass through the silica layer. Considering the pore size of the Vycor support (3.6 nm), this 10 nm thickness of the silica layer may be of the order of the smallest thickness level that can be achieved by the CVD technique. This thickness is much smaller than the thickness (500 nm) obtained by conventional CVD of silica [21].

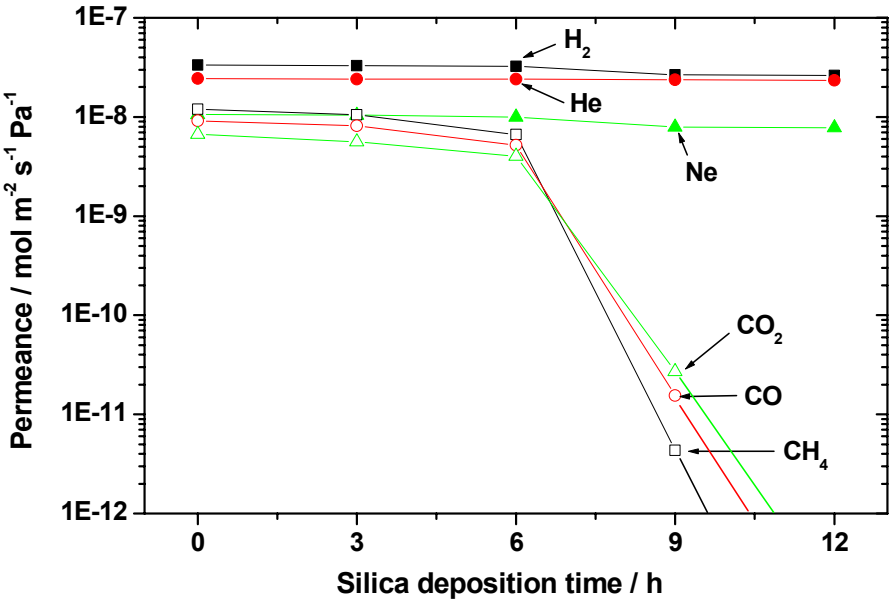

Figure 3.6. Gas permeance vs. silica deposition time

The temperature dependence of the permeance of He, Ne and H_2 on the Nanosil and the fresh Vycor are shown in Figure 3.7. The permeance through Vycor decreases with temperature over the entire range as expected from the Knudsen equation while the permeance through the Nanosil membrane shows an increase with temperature. These results indicate that the gas diffusion mechanism changed from Knudsen to an activated diffusion process in forming the Nanosil membrane. Only in the case of helium did the permeance decrease at the highest temperature. This was because the permeance approached that of the Vycor as the temperature increased over 673 K. This result is expected as the Nanosil membrane is in the form of a silica layer on top of the Vycor support and the permeance of helium on the Nanosil membrane is limited at high temperature by the Vycor support. The approach to such behavior for H_2 and Ne at temperature higher than 873 K is also seen in the data.

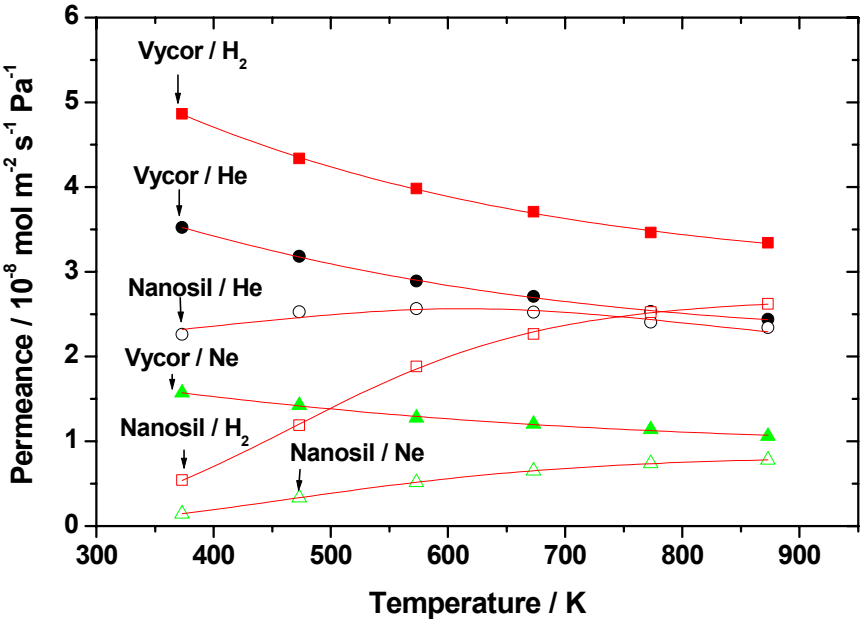

Figure 3.7. Temperature dependence of the permeance of He, Ne, and H_2

It is important to calculate the gas permeance of only the top silica layer in the Nanosil membrane, since the total permeance on the membrane could be improved using other supports that have higher permeance than the porous Vycor. The permeance of He, Ne, and H_2 on the silica layer can be obtained using a series analysis of gas diffusion, where the total resistance for gas permeation on the Nanosil membrane is a summation of the resistance on the Vycor support and the silica layer.

$$\frac{1}{Q_{\text{Nanosil}}} = \frac{1}{Q_{\text{Vycor}}} + \frac{1}{Q_{\text{silica}}} \tag{3.14}$$

where Q is the permeance (mol m^{-2} s^{-1} Pa^{-1}). Since the gas permeance of He, Ne and H_2 on the Vycor alone is known, the permeance on the top silica layer can be calculated. This is compared with the permeance on Vycor and Nanosil in Figures 3.8 – 3.10. The much higher permeance of the gases on the silica top layer clearly indicates that the permeance on the Nanosil membrane is limited by the permeance on the Vycor support.

The permeation characteristics of the small gas molecules on the silica layer were investigated by comparing them with the gas permeability on vitreous silica glasses reported in

the literature [22-27]. The structure of vitreous silica has been described as a disordered form of b-cristobalite that contains 5, 6, 7 and 8 membered rings, in which solubility sites are approximately 0.3 nm in diameter [28]. The structure of b-cristobalite is shown in Figure 3.11.

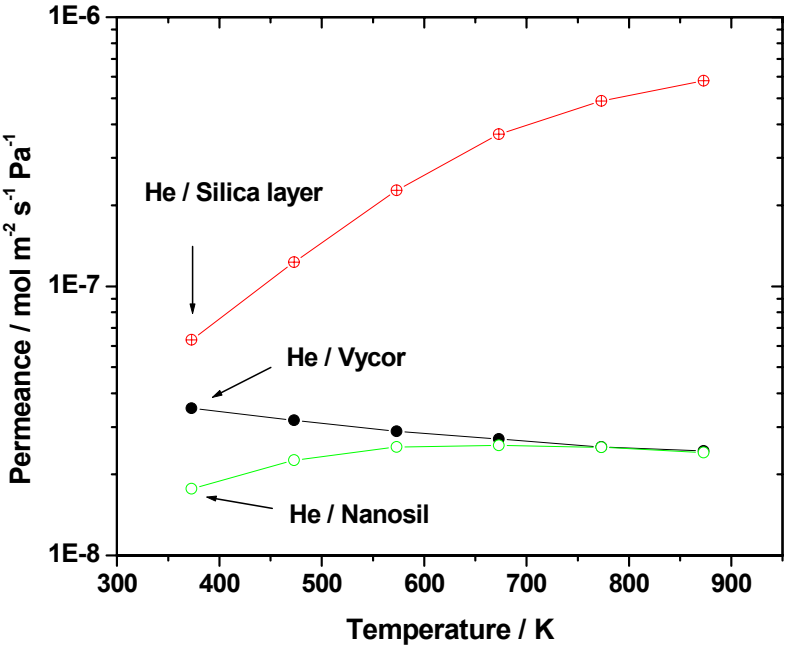

Figure 3.8. Model-calculated He permeance on the silica layer, and experimental permeance on the Vycor and Nanosil membranes

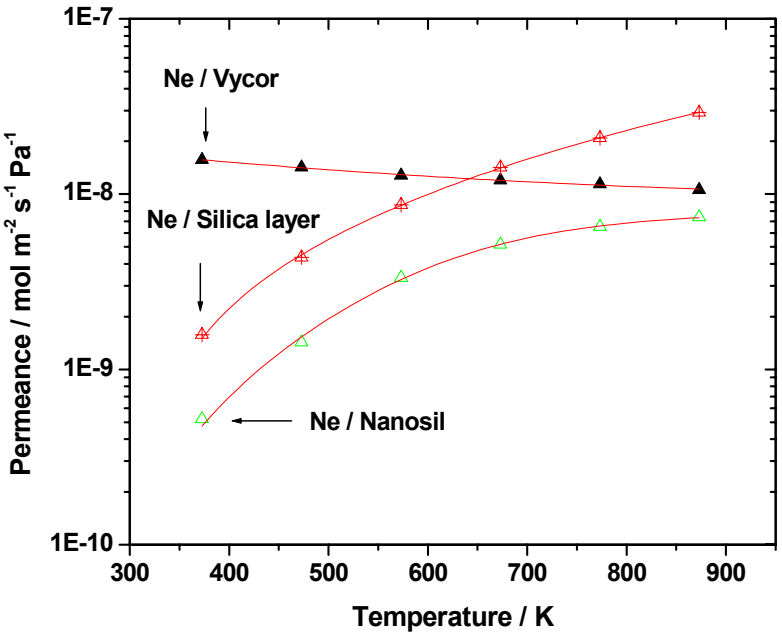

Figure 3.9. Model-calculated Ne permeance on the silica layer, and experimental permeance on the Vycor and Nanosil membranes

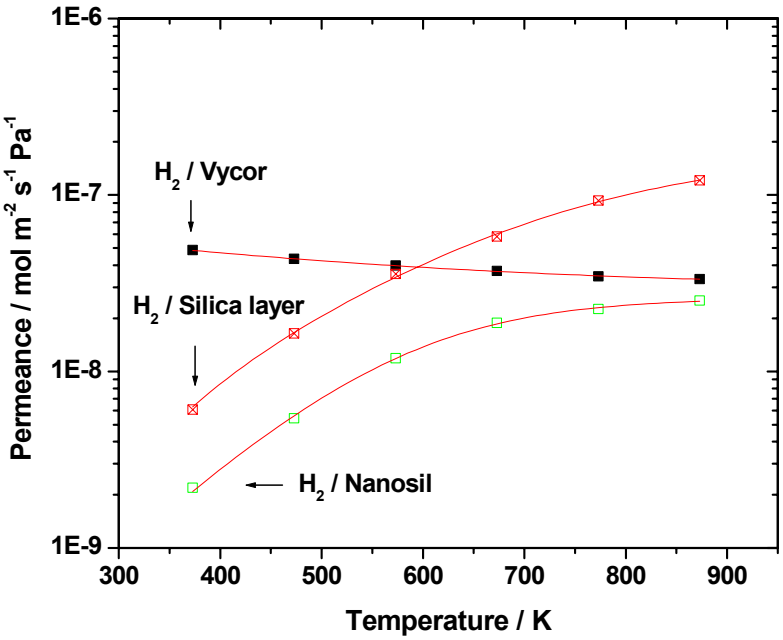

Figure 3.10. Model-calculated H_2 permeance on the silica layer, and experimental permeance on the Vycor and Nanosil membranes

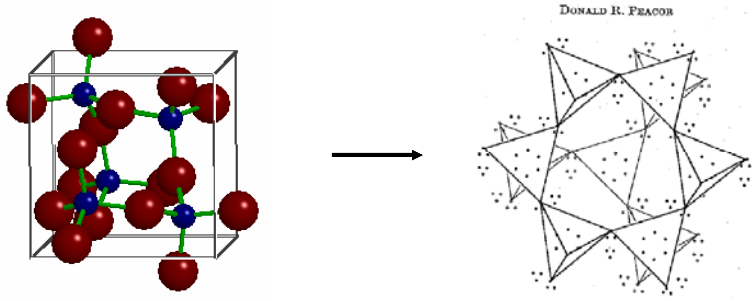

Figure 3.11. Structure of b-cristobalite

(6 membered silica ring is shown on the right side of the Figure)

This explains the size selectivity of the Nanosil membrane for the small gas species (He, Ne, and H_2) over the larger gas molecules (CH_4, CO and CO_2) in this work. The larger species simply do not fit in the solubility sites. The result is shown in Figure 3.12, where the permeability on the deposited silica layer was calculated based on the 10 nm thickness obtained from the AFM study and also corrected for the porosity ($\varepsilon = 0.28$) of the Vycor support. The calculation shows that the He, Ne and H_2 permeance on the deposited silica layer follows similar trends as on the vitreous silica glass with permeance in the order of He > H_2 > Ne. This order has been unexplained in the vitreous glass literature. It is highly unusual because it does not follow either the mass or size of the permeating species. A major difference is that the activation energies for the deposited silica layer are lower than for the vitreous silica. The activation energies of gas permeation on the silica layer and on vitreous glass are compared in Table 3.3. Similar results of low activation energy of permeance (6 – 35 kJ mol^{-1}) for hydrogen on supported silica membranes have been reported [29]. Considering the different synthesis conditions between the vitreous silica glass [30] and the silica layer obtained by CVD in this work, the lower activation energy of gas permeation clearly indicates a different pore structure in the SiO_2 matrix of the Nanosil membrane that allows for easier passage through the ring openings.

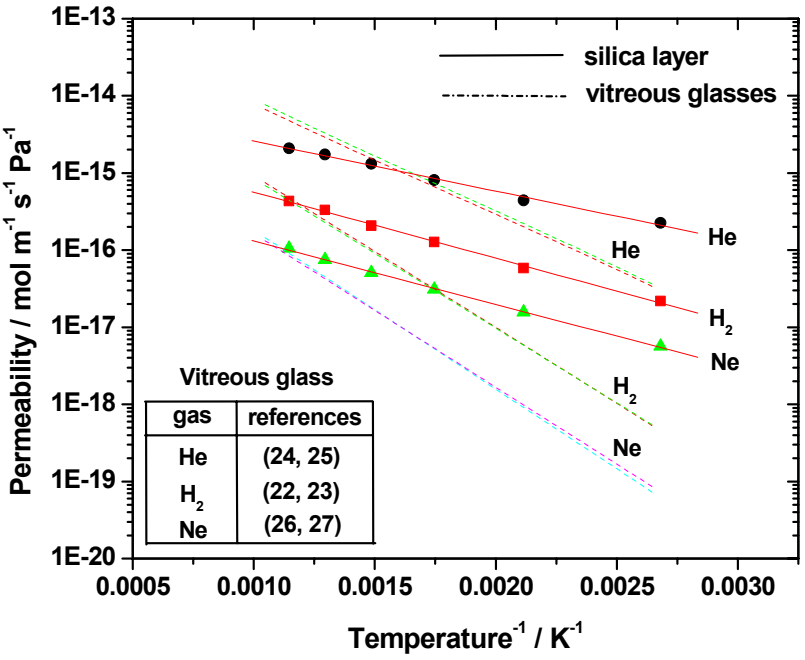

Figure 3.12. He, Ne, and H_2 permeability on the silica layer and vitreous glasses

Table 3.3. Activation energies on the deposited silica layer and vitreous silica glass

	Deposited silica layer E_a (kJ mol^{-1})	Silica Glass E_a (kJ mol^{-1})	Reference
He	12.4	17.8 – 21.1	24, 25
Ne	15.7	33.8 – 39.5	26, 27
H_2	16.4	37.2 – 38.8	22, 23

A final item that should be noted is that the permeance order of He, Ne and H_2 follows neither size nor mass of the molecules. This unusual order of gas permeance may be explained using the statistical gas permeance model on the vitreous silica glass (Eq. 3.12). The model indicates that the preexponential factor depends on the mass and vibrational frequency of

dissolved gas molecules at the doorway sites, and the number of solubility sites available per m^3 of glass volume. These are the variables that change with gas species whereas other parameters remain the same since they are geometric constants of the silica structure.

Classically the vibrational motion of an adsorbed molecule has been described assuming a harmonic oscillator where the vibrational frequency is given by,

$$\nu = \frac{1}{2\pi}\sqrt{\frac{f}{m}} \tag{3.15}$$

where f is a force constant. Values of the vibrational frequencies of dissolved gas molecules in solubility sites of silica glass have been reported in the literature where the values were obtained by fitting experimental gas solubility data to the statistical model equation (Eq. 3.11) [13,14]. The vibrational frequencies of He, Ne and H_2 were of the order of $10^{12} \sim 10^{13} s^{-1}$ (He $\nu = 6.90\times10^{12}$ s^{-1}, Ne $\nu = 4.38\times10^{12}$ s^{-1}, H_2 $\nu = 1.22\times10^{13}$ s^{-1} [14]).

The number of solubility sites available for gas species per unit volume of silica glass, N_s, plays an important role in the gas permeability. A theoretical calculation assuming that vitreous silica glass has a slightly disordered β-crystobalite has been reported in the literature [31] giving a value of $N_s = 2.22\times10^{28}$ sites m^{-3}. However, experimental studies have shown that the number of solubility sites in silica glass available for He, Ne and H_2 are different (He $N_s = 2.3\times10^{27}$ sites m^{-3} [32], Ne $N_s = 1.3\times10^{27}$ sites m^{-3} [32], H_2 $N_s = 1.07\times10^{27}$ sites m^{-3} [33]). This is because a size distribution exists for the solubility sites in silica glass and the different size of the gas molecules [34]. It indicates that the number of solubility sites available for gas species increases as the molecular size decreases.

The gas permeance on the silica layer of the Nanosil membrane was analyzed using the statistical permeance model (Eq. 3.12). The silica layer thickness, L, and the jump distance, d, used for the calculation were 10 nm and 0.3 nm respectively. The vibrational frequency (ν^*) of each gas species was taken to be the same as in glass and the activation energy for permeation (ΔE_K) and the number of solubility sites, N_s, available for each gas species were calculated. The model fitting was carried out using the Nelder-Mead simplex method. The fitting results are shown in Figure 3.13. They display excellent agreement between the model analysis and the

experimental data with a permeance order of He > H_2 > Ne, that is the same as that obtained experimentally.

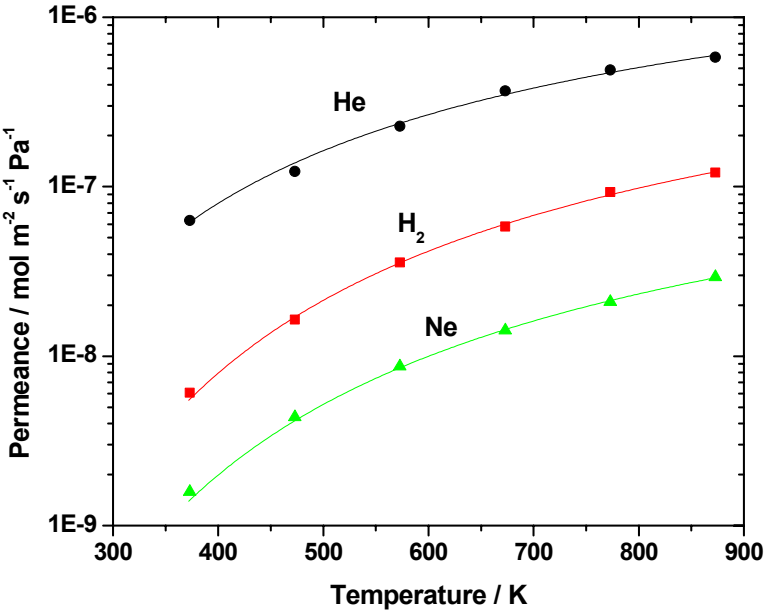

Figure 3.13. Statistical model calculated He, Ne, and H_2 permeance on the silica layer Points = Experimental values, Curves = Calculated values

The best-fit parameter values are summarized in Table 3.4. The calculated N_s values were 3.4×10^{27} sites m^{-3} for helium, 1.4×10^{27} sites m^{-3} for neon and 1.4×10^{27} sites m^{-3} for hydrogen, which were slightly higher than the corresponding values for glass. This makes sense since the structure of the membrane is expected to be more open and to accommodate more sites. The activation energies were also in good agreement with the measured values. The unusual order of permeability can now be understood. The higher permeability of He over H_2 is due to the larger number of solubility sites that can accommodate the smaller sized He. The higher permeability of H_2 over Ne is due to its smaller mass which results in a larger vibrational frequency.

Table 3.4. Values of the parameters for the statistical model analysis

	Number of solubility sites N_s (m^{-3})	Vibrational frequency ν* (s^{-1})	Activation energy E_a (kJ mol^{-1})	Sum of least squares $\Sigma (Q_{cal.} - Q_{expl.})^2$
He	3.41×10^{27}	6.90×10^{12}	9.7	1.20×10^{-15}
Ne	1.35×10^{27}	4.38×10^{12}	14.0	3.27×10^{-19}
H_2	1.37×10^{27}	1.22×10^{13}	13.6	1.82×10^{-17}

In summary, the model analysis was able to account for the unusual order of the small gas permeance on the silica layer of the Nanosil membrane, and gave physically realistic values for the solubility sites and activation energy for permeation.

3.5. Conclusions

The permeation characteristics of the gas molecules, He, Ne, H_2, CH_4, CO and CO_2, on the composite Vycor-supported silica membrane, referred to as Nanosil, were investigated. After 12 h of silica deposition on the Vycor support, the membrane showed at least a 10,000 fold higher hydrogen selectivity over the larger gas molecules, CH_4, CO and CO_2. The permeance of hydrogen on the Nanosil membrane was very high and comparable to the permeance on the fresh Vycor support (order of 10^{-8} mol m^{-2} s^{-1} Pa^{-1}) at 873 K. The gas permeance on the Nanosil membrane was activated and increased with temperature. However, this permeance was limited at high temperature because of the limited permeance on the Vycor support.

The gas transport characteristics on the Vycor and Nanosil membranes were discussed with relevant diffusion models. Surface diffusion enhanced Knudsen diffusion was a good model for the gas transport on the Vycor support. Gas transport on the deposited silica layer was successfully described by a statistical solid state diffusion model, which was able to account for the unusual permeation order He > H_2 > Ne, which did not follow mass or atomic size. Values

for solubility site densities ((1-3) $\times 10^{27}$ sites m^{-3}) and activation energies (10-14 kJ mol^{-1}) were physically realistic and matched experimental quantities.

References

[1] S.-T. Hwang, K. Kammermeyer, *Can. J. Chem. Eng.* **1996**, 44, 82.

[2] A.B. Shelekhin, A.G. Dixon, Y.H. Ma*, AIChE J.* **1995**, 41 (1), 58.

[3] A.J. Burggraaf, *J. Membr. Sci.* **1999**, 155, 45.

[4] R.M. Barrer, *J. Chem. Faraday Trans.* **1990**, 86 (7), 1123.

[5] J. Xiao, J. Wei, *Chem. Eng. Sci.* **1992**, 47 (5), 1123.

[6] R.S.A. de Lange, K. Keizer, A.J. Burggraaf, *J. Membr. Sci.* **1995**, 104, 81.

[7] V. Breger, E. Gileadi, *Electrochim. Acta,* **1971**, 16, 177.

[8] M. Bhandarkar, A.B. Shelekhin, A.G. Dixon, Y.H. Ma, *J. Membr. Sci.* **1992**, 75, 221.

[9] Y.H. Ma, Adsorption phenomena in membrane systems, in A.J. Burggraaf, L. Cot (Ed.), Fundamentals of inorganic membrane science and technology, Elsevier, Amsterdam, **1996**, pp. 36-42.

[10] I. Langmuir*, J. Am. Chem. Soc.* **1915**, 37, 1139.

[11] M. Knudsen, *Ann. Phys.* **1909**, 28, 75.

[12] J.S. Masaryk, R.M. Fulrath, *J. Chem. Phys.* **1973**, 59 (3), 1198.

[13] P.L. Studt, J.F. Shackelford, R.M. Fulrath, *J. Appl. Phys.* **1970**, 41 (7), 2777.

[14] J.F. Shackelford, P.L. Studt, R.M. Fulrath, *J. Appl. Phys.* **1972**, 43 (4), 1619.

[15] M. Mulder, Basic principles of membrane technology, Kluwer academic publishers, Dordrecht, 1996, pp. 227.

[16] T. Okubo, H. Inoue, *J. Membr. Sci.* **1989**, 42, 109.

[17] R.A. Levy, E.S. Ramos, L.N. Krasnoperov, A. Datta, J.M. Grow, *J. Mater. Res.* **1996**, 11 (12), 3164.

[18] C.E. Megiris, J.H.E. Glezer, *Ind. Eng. Chem. Res.* 1992, 31, 1293.

[19] C.N. Satterfield, T.K.Sherwood, The role of diffusion in catalysis, Addison-Wesley, Reading Mass. **1963**.

[20] D.W. Breck, Zeolite molecular sieves: structure, chemistry and use, John Wiley & Sons, New York, **1974**, pp. 636.

[21] M. Tsapatsis, G.R. Gavalas, *J. Membr. Sci.* **1994**, 87, 281.

[22] R.W. Lee, R.C. Frank, D.E. Swets, *J. Chem. Phys.* **1962**, 36, 1062.

[23] R.W. Lee, *J. Chem. Phys.* **1963**, 38, 448.

[24] J.E. Shelby, *J. Am. Ceram. Soc.* **1972**, 55 (2), 61.

[25] J.E. Shelby, *J. Am. Ceram. Soc.* **1972**, 54 (2), 125.

[26] J.E. Shelby, *J. Am. Ceram. Soc.* **1973**, 56 (6), 340.

[27] W.G. Perkins, D.R. Begeal, *J. Chem. Phys.* **1971**, 54 (4), 1683.

[28] R.M. Barrer, D.E.W. Vaughan, *Trans. Faraday Soc*. **1967**, 63, 2275.

[29] A.K. Prabhu, S.T. Oyama, *J. Membr. Sci.* **2000**, 176, 233.

[30] R.H. Doremus, Glass science 2nd Ed, John Wiley & Sons, New York, **1994**.

[31] T.F.W. Barth, E. Posnjak, *Z. Krist.* 1932, 81, 376.

[32] J.E. Shelby, *J. Appl. Phys.* **1976**, 47, 135.

[33] J.E. Shelby, *J. Appl. Phys.* **1977**, 48, 3387.

[34] J.F. Shackelford, J.S. Masaryk, *J. Non-crystalline Solids,* **1978**, 30, 127.